

# AN APPLICABILITY OF EQUIVALENT CRACKING ENERGY CONCEPT FOR IMPACT RESPONSE ANALYSIS OF RC GIRDERS

Abdul Qadir BHATTI\*<sup>1</sup>, Norimitsu KISHI\*<sup>2</sup>, Shinya OKADA\*<sup>3</sup> and Hisashi KONNO\*<sup>4</sup>

## ABSTRACT

Here, in order to establish a modification method for material properties of concrete so as to rationally analyze using coarse mesh, an equivalent fracture energy concept for concrete elements is proposed and the applicability was conducted comparing numerical analysis results with experimental results of falling weight impact loading test. From this study, it is confirmed that even though coarse mesh was used for prototype RC girder, similar results with those obtained using fine mesh can be assured and those results are in good agreements with the experimental ones.

**Keywords:** equivalent cracking energy, impact resistant design, impact response analysis, Drucker-Prager yield criterion, prototype RC girder

## 1. INTRODUCTION

The continuous expansion of urban zones in mountainous regions needs to establish the systems for protecting infrastructures from natural hazards such as snow avalanches, falling rocks, and landslides. In numerical analysis for estimating dynamic response behavior and/or sectional forces of the RC structures by means of FE method, mesh size may act very important role if cracking or tearing or penetration occurs in the concrete elements. However, considering the relationship between mesh size and material properties, rational response analysis method for precisely analyzing prototype RC structures under impact loading has not been established yet [1].

This work constitutes an effort directed towards the development of an objectivity algorithm for tensile failure of concrete elements based on the smeared cracking formulation. The algorithm has been implemented into LS-DYNA for hexahedron solid elements and correctly accounts for crack directionality effects [2]. Thus enabling the control of energy dissipation will be associated with each failure mode regardless of mesh refinement.

The advantage of the proposed technique is

that mesh size sensitivity on failure is removed leading to results, which converge to a unique solution, as the mesh is refined. The proposed algorithm has been validated by a full-scale prototype test using different cases of mesh refinement.

## 2. EXPERIMENTAL OVERVIEW

### 2.1 Dimensions and static design values

In this study, a RC girder, which is for designing roof of real RC rock-sheds, was taken for falling-weight impact test of prototype RC structures. The girder is of rectangular cross section and the dimensions are of 1 m x 0.850 m and clear span is 8 m long, which is similar to the width of real RC rock-sheds. Figure 1 shows dimensions of the RC girder, distribution of rebar, and measuring points for each response wave. In this figure, it is confirmed that 7#D29 rebars are arranged as main rebar assuming 0.64% of main rebar ratio corresponding to designing of real RC rock-sheds and 4#D29 rebars are arranged as the upper axial rebar to be about a half of main rebar ratio. Thickness of concrete cover is assumed to be 150 mm as well as real rock-sheds. D13 stirrups are arranged with intervals of 250 mm, which is less than a half of an effective height of

\*1 Graduate Student, Muroran Institute of Technology Japan, M.E., JCI Member

\*2 Prof., Dept. of Civil Engineering, Muroran Institute of Technology Japan, Dr.E., JCI Member

\*3 Researcher, Civil Engineering Research Institute (CERI) for Cold Region, M.E., JCI Member

\*4 Senior Researcher, Civil Engineering Research Institute (CERI) for Cold Region, Dr.E, JCI Member

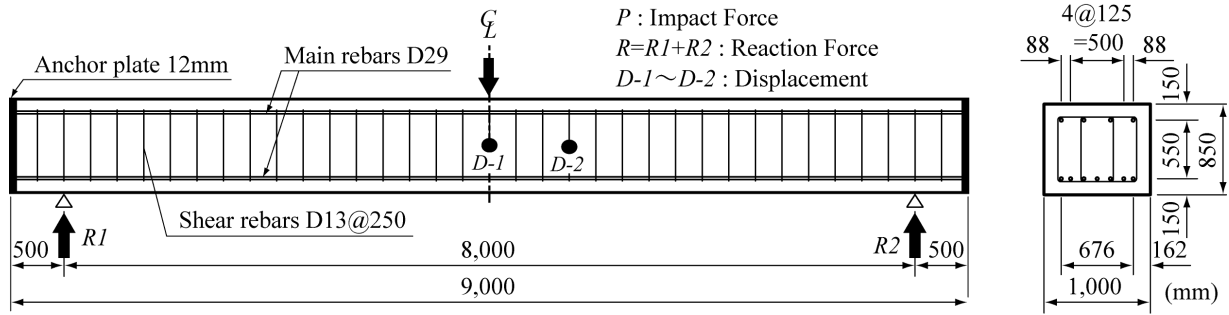


Fig. 1 Dimensions of RC girder and measuring items

the girder. In this study, arranging interlayer stirrups and upgrading in shear load-carrying capacity, the RC girder was designed to be collapsed with flexural failure mode. Axial rebars were welded to 12 mm steel-plates at the ends to save the anchoring length of the rebars.

The displacements of the girder were measured at mid-span  $D-1$  and  $D-2$  with the intervals of 750 mm from the mid-span. Impact force  $P$  was estimated using deceleration of the heavy weight, which is measured using accelerometer set at its top surface. Reaction force  $R$  ( $= R1+R2$ ) was also measured using load-cells installed in the supporting girdes. The detailed static design parameters of the RC girder are listed in Table 1. Static flexural and shear load-carrying capacities  $P_{usc}$  and  $V_{usc}$  were calculated based on Standard Specifications for Concrete Structures in Japan (JSCE, 2002) [3].

From this table, it is confirmed that the RC girder designed here will collapse with flexural failure mode under static loading because shear-bending capacity ratio  $\alpha$  is larger than unity. The static material properties of concrete and rebars during experiment are listed in Table 2.

## 2.2 Experimental method

In the experiment, a 2,000 kg heavy weight was lifted up to the prescribed height of 5 m by using the track crane, and then dropped freely to the mid-span of girder with a desorption device. A heavy weight is made from steel outer shell with 1 m in the diameter, 97 cm in height, and spherical bottom with 80 cm in radius and its mass is adjusted filling concrete and steel balls. RC girder was set on the supporting girdes, which are made so as to freely rotate but not to move toward each other. The ends of RC girders were fixed in the upward direction using steel rods and cross beams to prevent from jumping up at the time of impacted by a heavy weight. In this experiment, impact force wave ( $P$ ), reaction force wave ( $R$ ), and displacement waves ( $D$ ) at two

points near mid-span were measured. Impact force wave was estimated using a deceleration of heavy weight, which is measured using accelerometers set at the top-surface of weight. The accelerometer is of strain gauge type and its capacity and frequency range for measuring are 1,000 times gravity and DC through 7 kHz, respectively. Each load-cell for measuring reaction force are of 1,500 kN capacity and more than 1 kHz measuring frequency. For measuring displacements, laser-type variable displacement transducers (LVDTs) were used which are of 200 mm maximum stroke and 915 Hz measuring frequency. Analog signals from those sensors were amplified and converted to digital ones.

## 3. ANALYTICAL OVERVIEW

### 3.1 FE models

The purpose of this research is to propose the method for converting tensile strength of concrete element with arbitrary element size in span direction applying an equivalent fracture energy concept for full scale RC girder and the applicability is discussed by comparing with the experimental results. Therefore, the standard element division for precise numerical analysis result is needed. In this research, the suitable results were used and the standard analytical model such as MS35- $G_f$  was decided for prototype RC girder [4]. Similarly the standard mesh size of the span and the cross section width and height of the RC girder were set as 35 mm, 41 mm and 31 mm, respectively, based on the previous results [4].

On the other hand, four cases were considered by assuming 1, 3, 5, and 7 division for an interval of stirrup of 250 mm whose element sizes are 250 mm, 83 mm, 50 mm, and 35 mm, respectively and those cases are named as MS250- $G_f$ , MS83- $G_f$ , MS50- $G_f$  and MS35- $G_f$  respectively. For all cases, each mesh size along the girder near supporting area of 500 mm wide was set to be 35 mm long because of precisely

Table 1. Static design parameters of RC girder

Shear rebar ratio $\rho_t$	Static shear depth ratio $a/d$	Static shear capacity $V_{usc}$ (kN)	Static bending capacity $P_{usc}$ (kN)	Shear-bending capacity ratio $\alpha$
0.0064	5.71	1794	619.8	2.894

Table 2. Material properties of concrete and rebar

Type	Density $\rho$ (ton/m <sup>3</sup> )	Elastic coefficient $E$ (GPa)	Poisson's Ratio $\nu$	Yielding strength (MPa)
Concrete	2.343	25.4	0.177	31.2
Rebar D13	7.85	206	0.3	390
Rebar D29				400

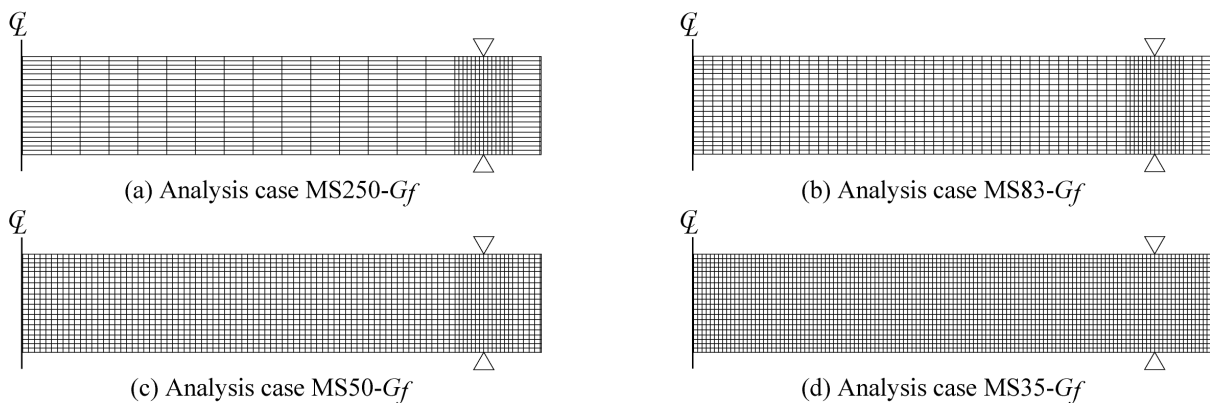


Fig. 2 FE mesh size distribution for each analytical case

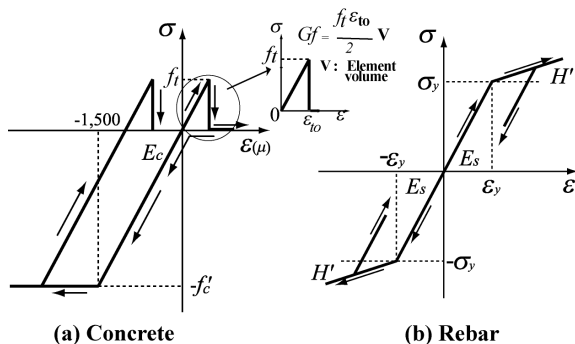


Fig. 3 Stress-strain relation of model

analyzing an interaction between supporting girdes and girders [1]. The mesh size distribution of each analytical case is shown in Fig. 2.

One quarter of RC girder were three dimensionally modeled for numerical analysis with respect to the two symmetrical axes. Figure 4 shows a mesh geometry of the girder, which is finally used for numerical analysis with optimum design accuracy were investigated here.

Geometrical configurations of the heavy weight and supporting gigue were also precisely modeled corresponding to the real ones. In this model, axial rebar and stirrup were modeled using beam element having equivalent axial stiffness, cross sectional area and mass with those

of real ones. The others were modeled using eight-node and/or six-node solid elements.

Total number of nodal points and elements for one-fourth model for MS35- $G_f$  are shown in Fig. 4 are 38,875 and 34,832, respectively. Number of integration points for solid and beam elements are one and four, respectively. In order to take into account of contact interface between concrete and head of heavy weight elements and between adjoining concrete and supporting gigue elements, contact surface elements for those were defined, in which contact force can be estimated by applying penalty methods for those elements but friction between two contact elements were neglected. Impact velocity of 9.8 m/sec for falling height of 5m was applied to all nodal points of the falling heavy weight. Based on the previous experience,  $h=1.5\%$  damping factor has been used for all cases of the numerical study [4].

### 3.2 Modeling of materials

The stress and strain relations of concrete and rebar are shown in Fig. 3. The outline of the material physical property models such as concretes, rebar is shown in Table 2. For the compression region, assuming that concrete is yielded at 1,500  $\mu$  strain, perfect elasto-plastic bilinear model was used. For the tension region,

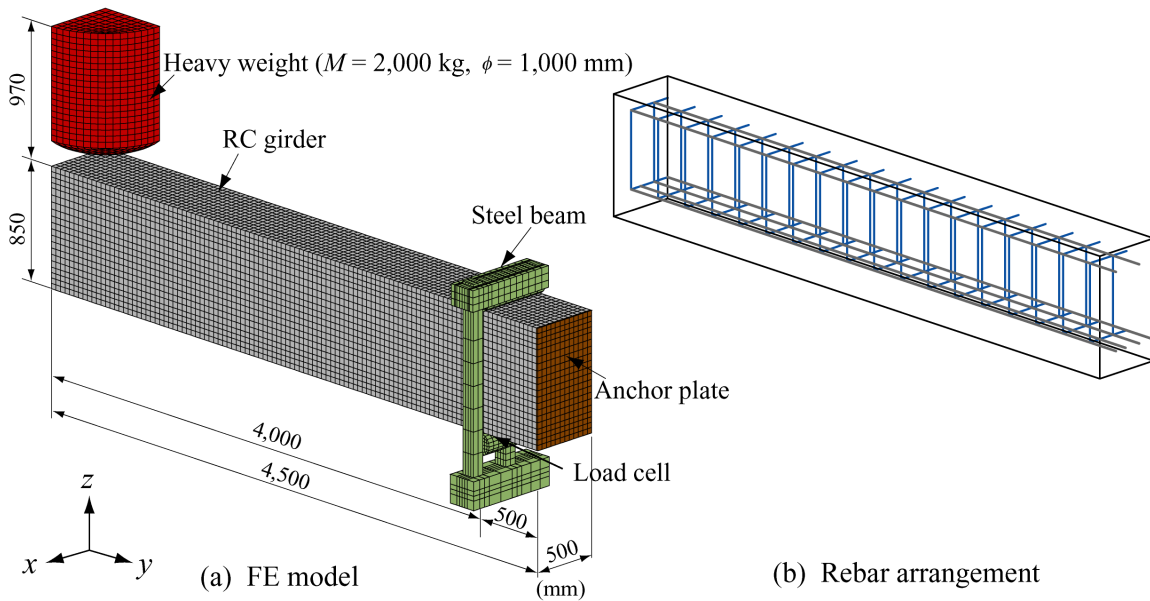


Fig. 4 FE Numerical analysis model

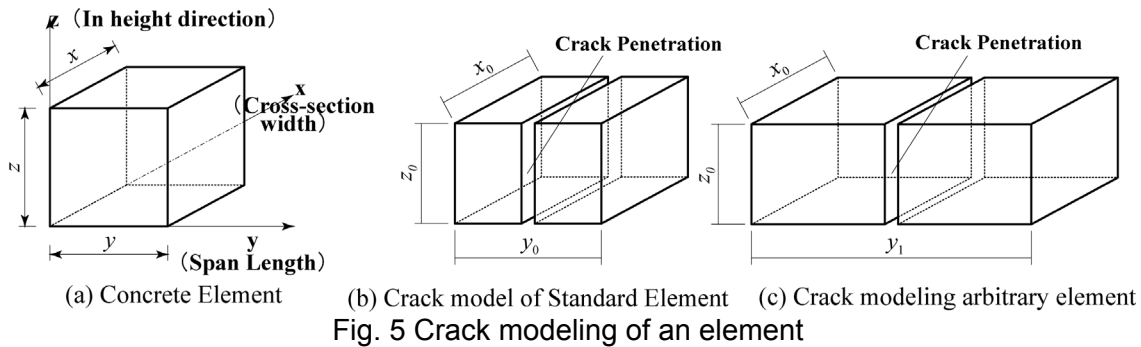


Fig. 5 Crack modeling of an element

Table 3. Tensile strength for different analytical cases

Element size in span direction (mm)	Fictitious tensile strength (MPa)
250	1.18
83	2.04
50	2.64
35	3.12

tensile strength of concrete is assumed to be one-tenth of compressive strength for the standard case of MS35- $G_f$  and MS35- $N$  but for other cases equivalent fracture energy concept was applied. Yielding of concrete has been judged based on the Drucker-Prager's yield criterion. Stress-strain relationship for main rebar and stirrup was defined using a bilinear isotropic hardening model. Plastic hardening coefficient  $H'$  was assumed to be 1% of Young's modulus  $E_s$ . Yield of rebar and stirrup was judged following von Mises yield criterion. Heavy weight, supporting girders and anchor plates for axial rebars set at the both ends of RC girder were

assumed to be elastic body because of no plastic deformation for those being found [5].

### 3.3 Equivalent fracture energy concept

In this paper, the element was assumed to be failed in the whole area of element because of applying smeared crack model, when negative pressure surcharged to the element reaches a tensile strength.

Assuming one flexural crack occurs in an element irrespective of magnitude of element size, the element must be set so as to be failed at the time when a strain energy stored in the element reaches the fracture energy which is the same among all concrete element size irrespective of magnitude of element size.

Based on this equivalent fracture energy concept, each concrete element can retain the equivalent fracture energy due to setting a fictitious tensile strength corresponding to volume of element. In Fig. 3(a), assuming fracture energy of standard concrete element and volume of the element as  $G_f$  and  $V_0$  respectively.  $G_f$  can be represented as Eq. 1 in which  $f_{t0}$  and  $\varepsilon_{t0}$

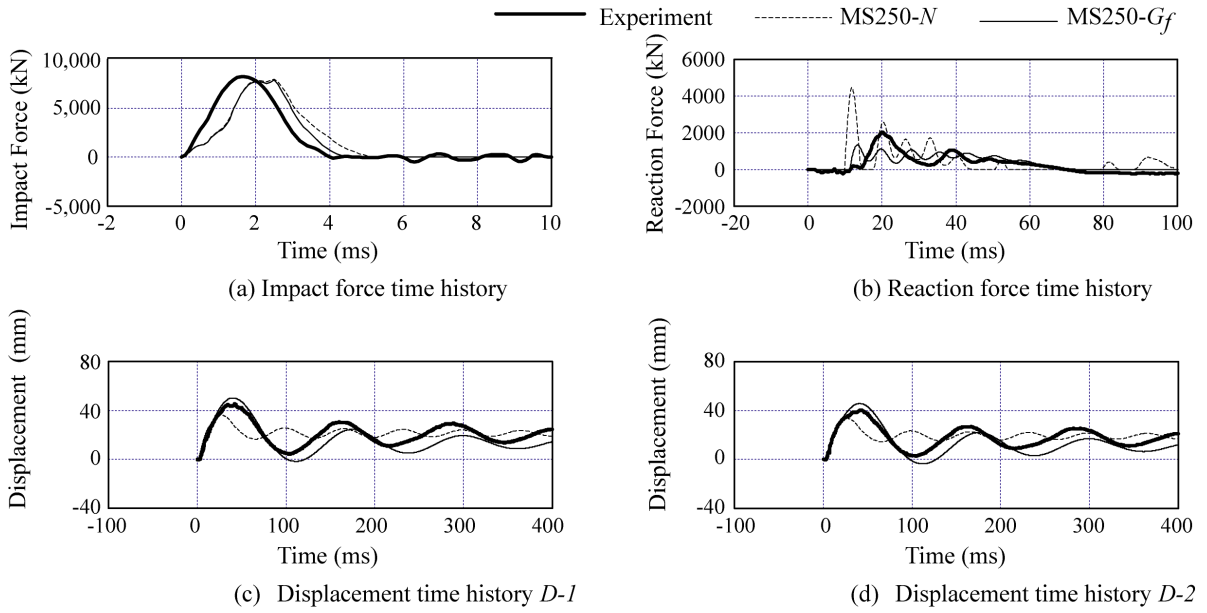


Fig. 6 Comparison between experimental and analysis results with/without  $G_f$

are tensile strength and strain at tensile failure of the standard concrete element as shown in Fig. 5.

$$G_f = \frac{f_{t0} \varepsilon_{t0}}{2} V_0 \quad (1)$$

Ultimate tensile strain  $\varepsilon_{t0}$  can be determined as the following equation described in Fig. 3(a),

$$\varepsilon_{t0} = \frac{f_{t0}}{E_c} \quad (2)$$

Assuming each element size in  $x$ ,  $y$  and  $z$  direction of the standard element as  $x_0$ ,  $y_0$ , and  $z_0$ , respectively, the volume of the standard element is as follows;

$$V_0 = x_0 y_0 z_0 \quad (3)$$

By putting the values of Eqs. 2 and 3, the fracture energy  $G_f$  can be obtained as,

$$G_f = \frac{f_{t0}^2}{2E_c} x_0 y_0 z_0 \quad (4)$$

Here, setting the fictitious tensile strength and element size in  $y$  direction of the  $i$ -element as  $f_{ti}$  and  $y_i$  and applying an equivalent fracture energy concept between standard element and  $i$ -element, following relationship can be obtained as;

$$\frac{f_{t0}^2}{2E_c} x_0 y_0 z_0 = \frac{f_{ti}^2}{2E_c} x_0 y_i z_0 \quad (5)$$

Fictitious tensile strength of  $i$ -element  $f_{ti}$  can be obtained as follows;

$$f_{ti} = f_{t0} \sqrt{\frac{y_0}{y_i}} \quad (6)$$

Therefore, taking the fictitious tensile strength  $f_{ti}$  obtained from Eq. 6 for  $i$  element with  $y_i$  as the size in  $y$ -direction, the crack occurred in the  $i$ -element can be rationally estimated similar

to  $f_{t0}$  of the standard element with fracture energy  $G_f$ . The fictitious tensile strength for each element size in  $y$ -direction used in this study is listed in Table 3.

#### 4. COMPARISON OF RESULTS

The applicability of the proposed method is examined for the set of each element length for different cases considering  $G_f$  in this section by comparing with experimental results. In Fig. 6., the MS250-N shows the analysis results for coarse mesh performed without considering the tensile strength as  $1/10^{\text{th}}$  of the compressive strength without considering  $G_f$ . The comparisons between results for coarse mesh with/without considering  $G_f$  are shown in Fig. 6. From Figs 6(a) and 6(b), it is understood that the impact force and reaction force wave cannot be much influenced by  $G_f$  factor. However, from Figs 6(c) and 6(d), it is observed that the displacement wave can be almost similar to the experimental results due to considering  $G_f$  factor.

In Figure 7, the applicability of the equivalent fracture energy concept has been compared with other mesh sizes having element length of 83 mm, 50 mm and 35 mm considering  $G_f$ . In Figs. 7(a) and 7(b) it is observed that the  $G_f$  factor has less influence on the time history of impact force and reaction force for other mesh sizes. However, the displacement wave can be considerably improved as shown in Figs 7(c) and 7(d). The maximum value of impact force wave is smaller than the experimental results regardless of the mesh size of the element length as previously observed. The maximum impact force

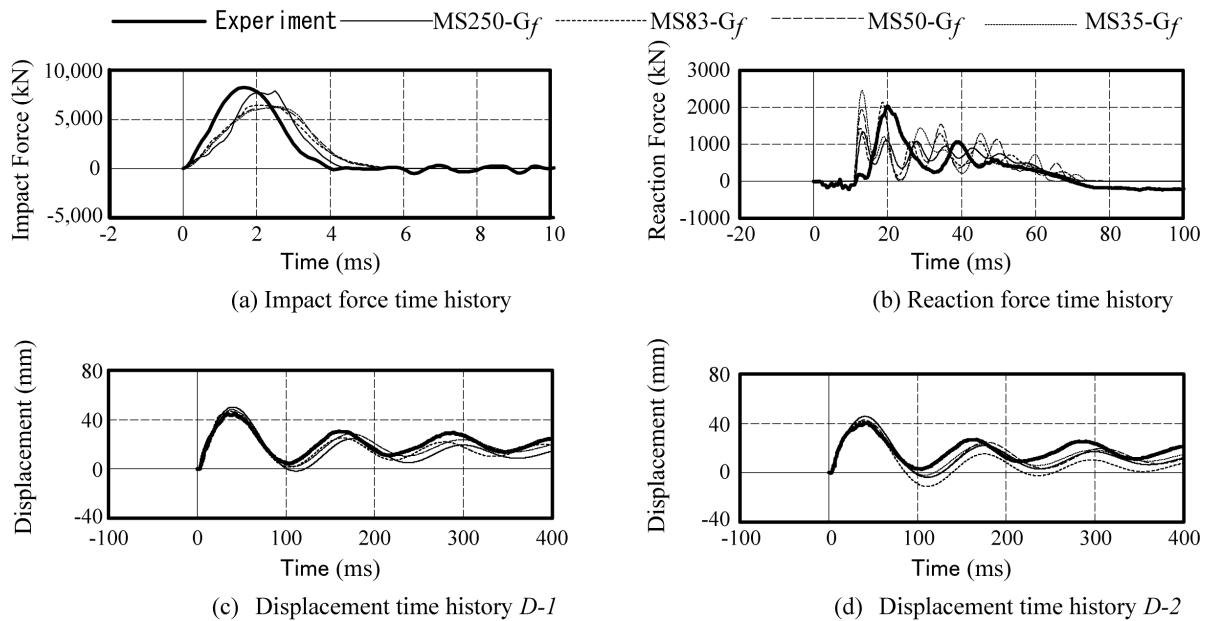


Fig. 7 Comparison between experimental and analysis results considering  $G_f$

indicates that the value in case of MS250- $G_f$  is the nearest to the experimental results. From Fig. 7(b), it is confirmed that the reaction force wave at the one supporting point tends to be high amplitude in case of one-division was almost similar to experimental one. It is understood that the amplitude of  $D-1/2$  as shown in Figs 7(c) and 7(d), the both frequency of displacement wave and the residual displacement are in the state of a free vibration after the maximum displacement regardless of the size of the element length by comparing the experimental results and the analytical one. By comparing the experimental results among four cases, the most underestimating case is MS83- $G_f$  though the level of the error margin is not large when seeing in detail.

## 5. CONCLUSIONS

In order to establish a modification method for material properties of concrete so as to rationally analyze using coarse mesh, an equivalent fracture energy concept for concrete element is proposed and the applicability was conducted comparing numerical analysis results with experimental results. From this study, it is confirmed that even though coarse mesh was used for RC girder, similar results with those obtained using fine mesh can be assured and are in good agreement with the experimental ones considering  $G_f$  concept. The results obtained from this study are as follows;

- (1) The fictitious tensile strength for coarse mesh has been proposed for the prototype

RC girder;

- (2) By using the fictitious tensile strength for coarse mesh with 250 mm mesh size, similar degree of accuracy can be obtained by using the fine mesh with mesh size of 35 mm; and
- (3) The maximum amplitude of impact force can be approximately obtained by using the coarse mesh size as 250 mm.

## REFERENCES

- [1] Kishi, N., Bhatti, A.Q., Okada, S., Konno, H., (2006). "An applicability of impact response analysis method for prototype RC girders under falling-weight impact loading" Journal of Structural Engineering, JSCE, 52A, 1261-1272.
- [2] Hallquist, J.O., (2000). "LS-DYNA User's Manual." Livermore Software Techn. Corp.
- [3] Japan Society of Civil Engineers (2002). "Standard Specifications for Concrete Structures-2002 "Structural Performance Verification" JSCE, (in English).
- [4] Bhatti, A.Q., Kishi, N., Konno, H. and Okada, S.: (2006). "Effective finite element mesh size distribution for proposed numerical method of prototype RC girders under falling-weight impact loading", Proceedings of 2<sup>nd</sup> International Conference on Design and Analysis of Protective Structures, Singapore, Nov 13-15, 261-272.
- [5] Bhatti, A.Q., Kishi, N., Konno, H. and Okada, S.: (2006) "An Impact Response Analysis of Large Scale RC Girder With Sand Cushion" Proceedings of JCI, Niigata, July 06, Vol. 28 No.2, 871-876.